PHYSICAL REVIEW B VOLUME 57, NUMBER 4 15 JANUARY 1998-II

Stability of Zr-Al alloys

M. Alatalo, M. Weinert, and R. E. Watson
Department of Physics, Brookhaven National Laboratory, Upton, New York 11973
(Received 14 October 1997)

The Zr-Al alloy system has one of the more complicated binary transition-metal aluminide phase diagrams: ten reported intermediate phases belonging to four different crystal systems. In order to understand the competition among different structures and concentrations, the heats of formation of a number of different possible structures were calculated using both all-electron and pseudopotential methods. The Zr_5Al_3 ($tI32$) and Zr_5Al_4 ($hP18$) phases are predicted to be high-temperature phases. The existence of the large number of observed phases is attributed to the fact that the heats of formation for Zr_xAl_{1-x} for $x=0.25-0.75$ fall on a nearly straight line, suggesting that these phases should have narrow composition ranges. In addition, a simple procedure to modify and test the pseudopotentials is presented and shown to yield calculated metallic alloy properties in good agreement with the all-electron results. [S0163-1829(98)50704-7]

Of all the transition metal aluminide binary phase diagrams, that of the Zr-Al system, shown schematically in Fig. 1, is one of the more complicated ones.[1,2] There are ten reported compounds at various concentrations, all of which experimentally are found to have extremely narrow concentration ranges, only on the order of 1%. Of these phases, two (Zr_5Al_3 and Zr_5Al_4) are high-temperature phases and a number of the others decompose into other phases at high temperatures. The phase diagram, which consists mainly of two-phase regions, is also rich in a structural sense:[3] the various compounds are found in hexagonal, orthorhombic, tetragonal, and cubic structures, with four of the phases representing prototype structures (see Table I). Because of these inherent structural differences, it is not possible to describe the different alloys as simple decorations of one underlying lattice.

The Zr-Al system is a rather severe test for electronic structure theory since it must describe not only the competition among different crystal structures at a given concentration, but also the competition among phases with different stoichiometries. In this paper we present the calculated heats of formation ΔH for all the reported phases, as well as a number of other plausible competing ones. We show that many of the observed features of the phase diagram can be understood in simple terms based on our calculated results.

An additional major objective of the present paper is to critically assess the ability of pseudopotential methods to describe the bonding of metallic alloys. While all-electron and pseudopotential calculations should agree in principle, in practice the particular choice of the pseudopotential may have significant effects on the calculated properties.

The all-electron calculations use the full-potential linearized augmented Slater-type orbital[4] (LASTO) method, while the pseudopotential calculations use an iterative method[5] described previously. The starting pseudopotentials were generated using the Troullier-Martins scheme[6] and put into a separable form by the Kleinman-Bylander[7] procedure. Rather than judging the quality of a pseudopotential by comparing with experiment directly (discrepancies could result from the choice of exchange correlation), a pseudopotential should be judged by its ability to reproduce the all-electron results; at best, pseudopotentials provide an approximation to the all-electron problem.

To test the Zr pseudopotential, the structural properties of bulk hcp Zr were calculated using both methods, with the same ranges of lattice constants, **k** points, etc. The calculated properties of hcp Zr obtained using standard pseudopotentials (including a nonlinear core correction) agreed with experiment to a level comparable to that found for other systems using the LDA. A more severe test, however, is provided by the fcc-bcc energy difference. Although only ~ 0.02 eV/atom, this energy difference is relevant to the competition among different phases. For a wide variety of different inputs to the pseudopotential (varying cutoff radii and configurations), the pseudopotential calculations gave the *wrong* ordering compared to the all-electron results.

To generate a better pseudopotential, we make use of the arbitrariness inherent in the pseudopotential itself. To reproduce the all-electron results, the pseudopotential is truncated in reciprocal space; this expansion then *defines* the pseudopotential. (The long-range Coulomb piece is not truncated, but is taken fully into account.) This approach has several advantages: (1) The pseudopotential is well-defined in both real and reciprocal space and remains constant independent of the wave-function cutoff. (2) The lattice parameters were

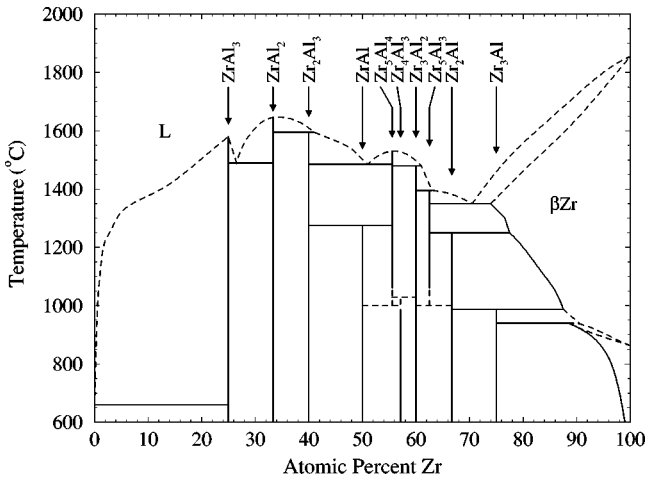

FIG. 1. Schematic phase diagram for Al-Zr based on those in Refs. 1 and 2.

TABLE I. Phases, crystal structures, and calculated heats of formation ΔH for Zr-Al alloys. The all-electron (pseudopotential) results are given in the column labeled ''LASTO'' (''PWPP''). [For Zr_4Al_3, the Zr $4p$ states have been treated both as band and as core states (Ref. 11).]

Phase	Crystal class	Structure type	ΔH (eV/atom) LASTO	PWPP
$ZrAl_3$	$tI16$	$ZrAl_3$	−0.47	−0.50
	$tI8$	$TiAl_3$	−0.44	−0.48
	$cP4$	Cu_3Au	−0.45	−0.47
$ZrAl_2$	$hP12$	$MgZn_2$	−0.56	−0.57
	$cF24$	$MgCu_2$		−0.56
	$tI24$	Ga_2Hf		−0.53
Zr_2Al_3	$oF40$	Zr_2Al_3	−0.50	−0.533
ZrAl	$oC8$	CrB	−0.45	−0.46
	$cP2$	CsCl	−0.27	−0.29
	$tP2$	CuAu-I	−0.43	−0.45
Zr_5Al_4	$hP18$	Ga_4Ti_5	−0.40	−0.42
Zr_4Al_3	$hP7$	Zr_4Al_3	−0.45	−0.47
	Semicore correction		−0.47	−0.42
Zr_3Al_2	$tP20$	Zr_3Al_2		−0.40
Zr_5Al_3	$hP16$	Mn_5Si_3		−0.35
	$tI32$	W_5Si_3	−0.35	−0.37
Zr_2Al	$hP6$	$InNi_2$	−0.35	−0.37
	$tI12$	Al_2Cu	−0.30	−0.31
Zr_3Al	$cP4$	Cu_3Au	−0.30	−0.31
	$cF16$	BiF_3	−0.12	−0.15
	$cP8$	A15	−0.23	−0.26

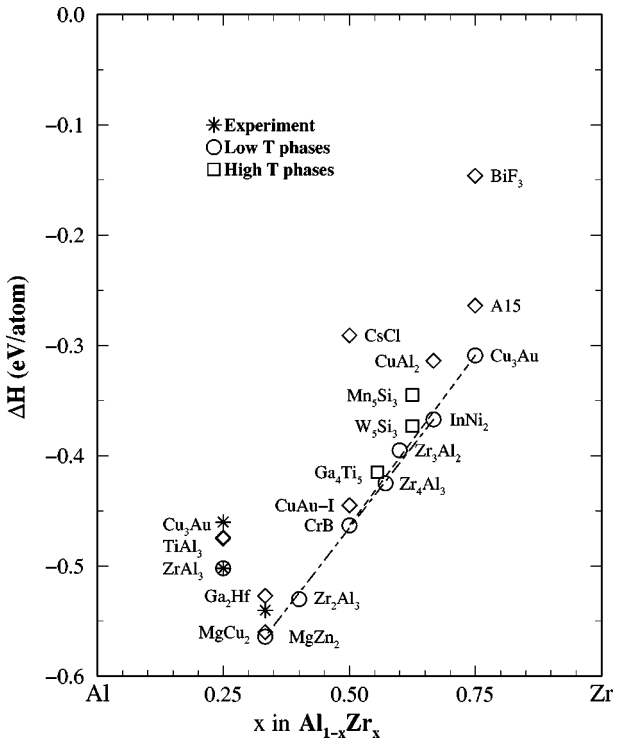

FIG. 2. Heats of formation for the Zr-Al alloys calculated using the pseudopotential method; experimental data are from Ref. 9. Energies are plotted to meV precision and the symbol size corresponds to approximately 0.01 eV.

found to be much less sensitive to changes in the plane wave cutoff for the wave functions used. The wave-function cutoff could be varied by more than a factor of 3 (up to 80 Ry) without significantly changing the lattice constant, in contrast to the standard pseudopotentials. (3) The fcc-bcc ordering was found correctly. The fcc-hcp difference, which is significantly larger, then agrees to better than 0.001 eV/atom between the two methods.

By varying the effective wave-function cutoff, the pseudopotential could be ''tuned'' (in the reciprocal space cutoff) to give the best possible agreement with the all-electron results, including lattice constants, bulk moduli, and energy differences. Note, however, this procedure requires an all-electron method to make direct comparisons with.

Using the Zr pseudopotential modified in this way (corresponding to an effective wave-function cutoff of 22 Ry), detailed comparisons of the structural properties were made between the pseudopotential and all-electron results for the alloys. As an example, for ZrAl along the CsCl to CuAu-I Bain distortion, there is excellent agreement for the calculated c/a ratios (1.364 vs 1.360) and the energy differences between the CsCl structure and the minimum (within 0.001 eV/atom). Likewise, both methods correctly give the orthorhombic CrB structure as the ground state at this concentration.

The small difference in energy between the CuAu-I and CrB structures ($\sim$0.02 eV/atom) highlights the need for full structural optimization, including the internal coordinates. (All heats reported for the the pseudopotential method are based on fully optimized structures. For four of the large unit-cell LASTO calculations, the internal parameter from the pseudopotential calculation were assumed.) Similarly, because the alloy phases are metallic and have different underlying structures, reciprocal space must be carefully sampled; depending on the structure, up to about 600 **k** points in the corresponding irreducible wedge of the Brillouin zone were used.

At each concentration, a number of different plausible structures are considered. While this approach might seem less systematic than, e.g., the cluster variation method[8] (CVM), these types of methods can only be applied to cases where the different configurations can be expressed as different decorations of the *same* underlying lattice. Since this is not the case for the Al-Zr alloys, the ''usual suspects'' approach is the only possible one when the relative energies of the different phases are needed to $\sim$0.01 eV/atom.

The calculated heats of formation for a number of different ordered alloys at different concentrations are given in Table I and the pseudopotential results are plotted in Fig. 2; the all-electron calculations give an effectively identical plot. Also shown in Fig. 2 are the few existing calorimetric measurements[9,10] on this system. The agreement between these data and the calculations is good and the lowest-energy structures (with the possible exception[11] of Zr_4Al_3) are consistent with the observed phases.

The pseudopotential values of ΔH are consistently larger in magnitude by a few hundredths of an eV than those obtained with LASTO, i.e., the pseudopotential calculation yields a stronger binding. Since the difference is approximately the same regardless of concentration, the two meth-

ods describe the bonding in slightly different ways. Two possible contributions are (1) the changes in the shape of the valence orbitals due to bonding are constrained by the core orthogonality requirement (for the pseudopotential method this constraint is not explicit), implying a somewhat smaller heat for the all-electron method, and (2) the tail functions of the LASTO basis set in the interstitial are less complete than the plane waves used in the pseudopotential calculations. Evidence supporting this latter explanation is that the heat of formation for ZrAl increases in magnitude by about 0.01 eV/atom when ''empty'' spheres are added to the holes in the more open CrB structure. While the small differences between the pseudopotential and LASTO results are probably combinations of these and other effects, the overall structure and physics obtained from both methods is the same.

The largest calculated ΔH is for $ZrAl_2$ in the hexagonal Laves structure, consistent with the pronounced skewing of the phase diagram shown in Fig. 1. For an ordered compound to be stable relative to a two-phase mixture of phases with different compositions, ΔH must lie below the line connecting the two competing phases. In Fig. 2, the tie lines from $ZrAl_2$ (hexagonal Laves structure) to Zr_2Al ($InNi_2$) and from ZrAl (CrB) to Zr_3Al (Cu_3Au) are shown. Although these lines (and the other tie lines in this region) are almost collinear, there is some curvature so that the observed low temperature phases are predicted to be stable.[11] The two observed high-temperature phases, Zr_5Al_4 and Zr_5Al_3, both clearly lie above the tie lines but by an amount that is small on an absolute scale ($\sim$300 K), as necessary if they are to be high-temperature phases.

Since heats of the low-energy phases fall all on a nearly common line, small changes in stoichiometry (antisite defects, etc.) will cause the energy of a phase to increase relative to its neighbors and rise above the tie lines. Thus, we would predict that the concentration ranges for the different line compounds are quite narrow and that the phase diagram consists mainly of two phase regions, in agreement with experiment. Further supporting evidence comes from the observation[12] that the existence of certain phases such as ZrAl depends strongly on the experimental conditions. The large number of observed phases is in some sense accidental in that slight changes in the electronic structure will cause ΔH of certain phases to shift, causing phases to disappear. (A decrease in binding energy of a phase will cause it to disappear, while an increase in binding may suppress neighboring phases.) Supporting this argument is the fact that the phase diagrams of the isoelectronic systems[2] Ti-Al and Hf-Al are roughly similar to Zr-Al, but both have fewer observed phases.

Our results for the structural parameters such as lattice constants, c/a ratios, and internal coordinates are generally in good agreement with the existing experimental data,[3] although little overall is known experimentally, especially concerning the internal coordinates. Although the high-temperature Zr_5Al_3 phase has been reported in both the $hP16$ (Mn_5Si_3) and $tI32$ (W_5Si_3) structures, our results clearly favor the $tI32$ form and are consistent with the suggestion[13] that the $hP16$ phase is stabilized by oxygen. The stability of the $tI32$ phase relative to the competing Zr_3Al_2 ($tP20$) and Zr_2Al ($hP6$) phases at high temperatures at least partially results from electronic entropy effects since this phase has a high peak in the density of states at the Fermi level. In the case of Zr_5Al_4, there is no corresponding large peak and this phase is most likely stabilized by vibrational entropy and configurational entropy associated with thermal activated defects such as vacancies, interstitials, and antisite defects.

The Al-Zr bond is relatively strong, thus favoring structures with unlike neighbors. Because the intrinsic size, as measured by the elemental volumes, of Zr is significantly ($\sim$50%) larger than Al, the standard close-packed structures give a poor filling of space and would cause the Al-Al, Zr-Al, and Zr-Zr bond lengths to all be similar. Thus, crystal structures that have sites with different sizes should be preferred. Arguments based on the size mismatch can be used to rationalize the occurrence of the CrB, rather the CuAu-I, structure for ZrAl. The calculated lattice parameters of these different structures are to a large extent determined by the Zr-Al bond lengths and volume conservation. The CrB structure, as opposed to CuAu-I, permits the Zr-Zr and Al-Al bond lengths to differ, allowing the number of near neighbors of the two atomic species to differ: Zr has 13 neighbors (6 Zr, 7 Al), while Al has 11 (7 Zr, 4 Al), and both the Zr-Zr and Al-Al distances are more representative of their ''natural'' separations. Thus, the CrB structure can better accommodate the different atomic sizes, while still maximizing Zr-Al bonding. Although size effects as such are difficult to quantify based on electronic structure calculations, the consequences of the size differences can be seen. In the present case, the changes in bonding between the CrB and CuAu-I structures cause the Fermi level of the CuAu-I phase to be about 0.19 eV higher than for CrB. A simple estimate of the change in the sum of one-electron energies yields a difference in binding of about 0.02 eV/atom, in almost perfect agreement with the full calculation.

Size is also an issue in a number of other structures in the Zr-Al system, including the existence of the Laves phase for $ZrAl_2$ with its 12- and 14-fold coordinated sites. The small difference in energy between the cubic and hexagonal Laves is related to band filling and to the additional freedom associated with relaxation of the c/a ratio and internal parameters, analogously to the fcc-hcp case. Similarly, for $ZrAl_3$ the antiphase $tI16$ ($D0_{23}$) structure at the ideal c/a ratio has a heat of formation of about 0.007 eV/atom less bound than those of the $TiAl_3$ and Cu_3Au structures. (The calculated difference in ΔH between the Cu_3Au and $ZrAl_3$ structures is about 0.027 eV/atom, in excellent agreement with the value[14] of 0.023 eV/atom extracted from studies of mechanical alloying.) While the stabilization of these antiphase structures has been attributed to purely electronic effects,[15] the relaxations induced by size effects play an essential role in modifying the electronic structure. Finally, the structures that occur, although of completely different symmetries and crystal classes, have some common features, in particular, many of the structures can be constructed using (possibly overlapping) hexagonal-like Zr-Al building blocks that can accommodate size mismatch between Zr and Al.

In conclusion, first-principles calculations of the heats of formation are able to explain the main features of the complicated Zr-Al alloy phase diagram, including the delicate competition among phases at different concentrations. The large number of phases is attributed to the nearly linear be-

havior of the heats of formation for the Zr-rich alloys and the existence of particular crystal structures are in part due to the size difference between Zr and Al. Finally, we have demonstrated that by using the arbitrariness inherent in pseudopotentials, the all-electron results for bulk systems can be reproduced and that these pseudopotentials can then be used to describe the bonding in metallic alloys.

We thank R. Podloucky for discussions. This research was supported by the Division of Materials Sciences of the U.S. Department of Energy (DOE) under Contract No. DE-AC02-76CH00016, by the DOE High Performance Computing and Communications Program, and used resources of the National Energy Scientific Computing Center, which is supported by the DOE Office of Energy Research.

[1] D. J. McPherson and M. Hansen, Trans. Am. Soc. Met. **46**, 354 (1954); M. Pöstchke and K. Schubert, Z. Metallkd. **53**, 549 (1962); J. Murray, A. Peruzzi, and J. P. Abriata, J. Phase Equil. **13**, 277 (1992); A. Peruzzi, J. Nucl. Mater. **186**, 89 (1992).

[2] T. Massalski, *Binary Alloy Phase Diagrams*, 2nd ed. (American Society for Metals, Metals Park, OH, 1990); B. Predel, in *Phase Equilibria Crystallographic and Thermodynamic Data of Binary Alloys*, edited by O. Madelung, Landolt-Börnstein New Series, Group IV, Vol. 5, Pt. a (Springer-Verlag, Berlin, 1991).

[3] P. Villars and L. D. Calvert, *Pearson's Handbook of Crystallographic Data for Intermetallic Phases*, 2nd ed. (American Society for Metals, Metals Park, OH, 1991).

[4] G. W. Fernando, J. W. Davenport, R. E. Watson, and M. Weinert, Phys. Rev. B **40**, 2757 (1989).

[5] N. Chetty, M. Weinert, T. S. Rahman, and J. W. Davenport, Phys. Rev. B **52**, 6313 (1995).

[6] N. Troullier and J. L. Martins, Phys. Rev. B **43**, 1993 (1991).

[7] L. Kleinman and D. M. Bylander, Phys. Rev. Lett. **48**, 1425 (1982).

[8] R. Kikuchi, Phys. Rev. **81**, 988 (1951); see also D. de Fontaine, Solid State Phys. **34**, 73 (1979).

[9] S. V. Meschel and O. J. Kleppa, J. Alloys Compd. **191**, 111 (1993); O. J. Kleppa, J. Phase Equil. **15**, 240 (1994).

[10] Because the heats derived from vapor pressure measurements (Ref. 12) have inherently large error bars and are in poor agreement with the calorimetric measurements for the Al-rich alloys, they have not been shown. (For the Zr-rich alloys, the agreement between these and the calculated values is reasonably good, on the order of a few hundredths of an eV/atom.)

[11] Even though Zr_4Al_3 is a prototype, its actual structure (Ref. 3) is still uncertain. Regardless of the experimental situation, ΔH (and the bulk modulus) obtained from both methods is out of line compared to *all* other calculated phases and would suppress a number of other phases. Because the Zr atoms in this structure have closer approaches than the other crystal structures, core-core repulsion of the Zr $4p$ levels may be underestimated. Full-potential linearized augmented plane wave calculations [R. Podloucky, M. Weinert, R. E. Watson, and M. Alatalo (unpublished)] were used to correct the pseudopotential results given in Table I and Fig. 2. Analogous LASTO calculations, however, show an increase in binding; this discrepancy is still unresolved.

[12] R. J. Kematick and H. F. Franzen, J. Solid State Chem. **54**, 226 (1984).

[13] L. E. Edshammar, Acta Chem. Scand. **16**, 20 (1960).

[14] P. B. Desch, R. B. Schwarz, and P. Nash, J. Less-Common Met. **168**, 69 (1991).

[15] A. E. Carlsson and P. J. Meschter, J. Mater. Res. **4**, 1060 (1989).